Published in final edited form as:
J Pineal Res. 2010 March ; 48(2): 157–169. doi:10.1111/j.1600-079X.2009.00739.x.

The inhibition of apoptosis by melatonin in VSC4.1 motoneurons exposed to oxidative stress, glutamate excitotoxicity, or TNF-α toxicity involves membrane melatonin receptors

Arabinda Das[1], **Misty McDowell**[1], **Matthew J Pava**[1], **Joshua A. Smith**, **Russel J. Reiter**[2], **John J. Woodward**[1], **Abhay K. Varma**[1], **Swapan K. Ray**[3], and **Naren L. Banik**[1,*]

[1] Department of Neurosciences (Division of Neurology), Medical University of South Carolina, Charleston, SC 29425, USA

[2] Department of Cellular and Structural Biology, University of Texas, San Antonio, TX 78229, USA

[3] Department of Pathology, Microbiology, and Immunology, University of South Carolina School of Medicine, Columbia, SC 29209, USA

Abstract

Loss of motoneurons may underlie some of the deficits in motor function associated with CNS injuries and diseases. We tested whether melatonin, a potent antioxidant and free radical scavenger, would prevent motoneuron apoptosis following exposure to toxins and whether this neuroprotection is mediated by melatonin receptors. Exposure of VSC4.1 motoneurons to either 50 μM H_2O_2, 25 μM glutamate (LGA), or 50 ng/ml tumor necrosis factor-alpha (TNF-α) for 24 h caused significant increases in apoptosis, as determined by Wright staining and ApopTag assay. Analyses of mRNA and proteins showed increased expression and activities of stress kinases and cysteine proteases and loss of mitochondrial membrane potential during apoptosis. These insults also caused increases in intracellular free [Ca^{2+}] and activities of calpain and caspases. Cells exposed to stress stimuli for 15 min were then treated with 200 nM melatonin. Post-treatment of cells with melatonin attenuated production of reactive oxygen species (ROS) and phosphorylation of p38, MAPK, and JNK1, prevented cell death, and maintained whole-cell membrane potential, indicating functional neuroprotection. Melatonin receptors (MT1 and MT2) were upregulated following treatment with melatonin. To confirm the involvement of MT1 and MT2 in providing neuroprotection, cells were post-treated (20 min) with 10 μM luzindole (melatonin receptor antagonist). Luzindole significantly attenuated melatonin-induced neuroprotection, suggesting that melatonin worked, at least in part, via its receptors to prevent VSC4.1 motoneuron apoptosis. Results suggest that neuroprotection rendered by melatonin to motoneurons is receptor mediated and melatonin may be an effective neuroprotective agent to attenuate motoneuron death in CNS injuries and diseases.

Keywords

apoptosis; cytoprotective; glutamate; H_2O_2; melatonin; motoneurons; TNF-α

[*]Correspondence to: Naren L. Banik, Department of Neurosciences, Medical University of South Carolina, 96 Jonathan Lucas Street, Charleston, SC 29425. Phone: (843) 792-8570; Fax: (843) 792-8626; Naren L. Banik (baniknl@musc.edu).

Introduction

Melatonin (*N*-acetyl-5-methoxytryptamine), a secretory product of the pineal gland, possesses a wide spectrum of biological effects and has been detected in many tissues [1–5]. It is highly lipophilic, which allows it to cross cell membranes easily and to reach all subcellular compartments, including mitochondria [3–5]. Melatonin reduces oxidative stress through its free radical scavenging effect and by indirectly increasing antioxidant enzyme activity [6]. With respect to its therapeutic potential, melatonin modulates the immune response [7,8], possesses anti-proliferative effects on tumor cells [8,10], and displays cytoprotective properties in normal cells [11–13].

Melatonin prevents neuronal cell death in a large number of neurodegeneration models [12–16]. Melatonin has low toxicity, even at very high concentrations [17]. The cytoprotective effect of melatonin is especially interesting for three major reasons. Melatonin easily crosses the blood-brain-barrier [18] allowing it to be administered either orally or intravenously. In addition, the fall in nocturnal melatonin blood level that is accentuated with increasing age parallels quite closely the appearance of chronic neurodegenerative disorders suggesting that the lack of melatonin in the elderly may contribute to the appearance of these diseases [19]. And finally, patients treated with high doses of melatonin do not experience any harmful side effects [20]. On the basis of these findings, melatonin has been proposed as a possible preventive treatment against neurodegenerative disorders.

The mechanisms involved in the neuroprotection provided by melatonin, however, remain unknown. The wide range of potential signal transducers, as well as the fact that it has non-receptor-mediated actions, accounts for the wide spectrum of melatonin's biological effects. Melatonin has at least two pertussis toxin-sensitive G-coupled membrane receptors, MT1 and MT2. Melatonin is also an antagonist of the Ca^{2+}-calmodulin complex (CaCaM) [21] and has both direct and indirect antioxidant properties [12,22]. Melatonin regulates the activation of several transcription factors (e.g., NF-κB, AP-1) [23,24] and activates ROR/RZR nuclear orphan receptor [25]. Moreover, binding sites for melatonin may exist in mitochondria [26,27] where it activates mitochondrial complexes I and IV. It also seems to bind to inactivate the mitochondrial permeability transition pore, thus preventing cytochrome *c* release and excitotoxic NMDA-induced cell death in cultures of striatal neurons [28]. Finally, a third type of melatonin receptor (MT3), which is cytosolic [29], has been identified in amphibia and birds, but its role in signal transduction is still unclear. However, MT3 sites, which lead to phosphatidylinositol turnover, can simultaneously function as quinone reductase 2.

Melatonin protects neuronal cells from injury through signal transduction pathways by the activation of the PI3-K/Akt survival pathway [30–32]. Although previous studies have demonstrated the neuroprotective effects of melatonin, its mechanisms have not been clearly elucidated. Oxidative stress, glutamate-induced excitotoxicity, and tumor necrosis factor-α (TNF-α)-induced cytotoxicity have been suggested to play a key role in most forms of neurodegeneration, including ischemic brain damage, trauma, Alzheimer's disease, alcoholic degeneration, and other diseases [33].

In this report, we studied the intracellular pathways involved in neuroprotection provided by melatonin against oxidative stress, glutamate excitotoxicity, and TNF-α toxicity in the VSC4.1 motoneuron cell line. Our findings indicate that the neuroprotection rendered by melatonin is mediated via its membrane receptors.

Materials and methods

Cell culture

Ventral spinal cord 4.1 (VSC4.1) motoneurons were grown in a monolayer to subconfluence in 75-cm^2 flasks containing 10 ml of DMEM/F12 medium with 15 mM HEPES, pyridoxine, and $NaHCO_3$ (Sigma, St. Louis, MO), supplemented with 2% Sato's components, 1% penicillin, streptomycin (Gibco-Invitrogen, Grand Island, NY), and 2% heat-inactivated fetal bovine serum (Hyclone, Logan, UT). Optimal doses of H_2O_2, glutamate, TNF-α (Sigma) and melatonin (Sigma) were determined for VSC4.1 cells. Cells were treated with 50 μM H_2O_2, 25 μM glutamate (LGA), and 50 ng/ml TNF-α alone and with 15 min 50 μM H_2O_2, 25 μM glutamate (LGA), and 50 ng/ml TNF-α treatment followed by post-treatment with either melatonin (100 nM) or melatonin + luzindole (10 μM) (Sigma). Cells were grown in an incubator at 37°C with 5% CO_2 and full humidity. Cells were collected after 24 h treatments.

Trypan blue dye exclusion test for residual cell viability after treatments

Following H_2O_2, LGA, TNF-α, melatonin, luzindole, and melatonin + luzindole treatments, the viability of attached and detached cell populations was estimated by trypan blue dye exclusion test. Viable cells did not take up trypan blue and maintained membrane integrity. Dead cells with compromised cell membranes took up trypan blue. At least 500 cells were counted in 4 different fields. The percentage of residual cell viability was calculated using the following formula: percentage of residual cell viability = [number of trypan blue negative cells/(number of trypan blue positive cells + number of trypan blue negative cells)] × 100.

Electrophysiological recordings for determination of whole-cell membrane potentials

Membrane potentials were recorded by the whole-cell patch-clamp electrophysiology using an Axopatch 200B amplifier (Molecular Devices, Sunnyvale, CA) in conjunction with AxographX software (Sydney, NSW). VSC4.1 cells on 35-mm culture dishes were perfused at room temperature with extracellular recording solution containing 135 mM NaCl, 5 mM KCl, 1.8 mM $CaCl_2$, 10 mM glucose, and 5 mM HEPES (pH adjusted to 7.2 with NaOH and osmolarity to 325 mOsM with sucrose). Patch electrodes (2.5 – 4.0 mOhms) were filled with an internal solution containing 150 mM KCl, 2.5 mM NaCl, 4 mM Mg-ATP, 2 mM Na-ATP, 0.3 mM Na-GTP, 5 mM Na-phosphocreatine, 10 mM HEPES (pH adjusted to 7.4 with NaOH and osmolarity to 310 mOsM with sucrose). The liquid junction potential was 4.1 mV and corrected for in all recordings. After seal formation and breakthrough in voltage-clamp (holding potential -60 mV), the amplifier was switched to current-clamp mode with zero holding current, and the resulting membrane potential was recorded.

Wright staining and ApopTag assay

Cells from each treatment were collected and washed with 1xPBS, pH 7.4, and sedimented onto the microscopic slide and fixed [34–36]. The morphological (Wright staining) and biochemical (ApopTag assay) features of apoptosis were examined, as described previously [34]. After Wright staining and ApopTag assay, cells were counted under the light microscope to determine percentage of apoptosis.

Fura-2 assay for determination of intracellular free [Ca^{2+}]

The level of intracellular free [Ca^{2+}] was measured using the fluorescence Ca^{2+} indicator fura-2/AM, as described previously [34–36]. The value of K_d, a cell-specific constant, was determined experimentally to be 0.164 μM for the VSC4.1 motoneurons cells, using

standards of the Calcium Calibration Buffer Kit with Magnesium (Molecular Probes, Eugene, OR).

Analysis of mRNA expression

Extraction of total RNA, reverse transcriptase-polymerase chain reaction (RT-PCR), and agarose gel electrophoresis were performed, as described previously [35,36]. All primers (Table 1) for the RT-PCR experiments were designed using Oligo software (National Biosciences, Plymouth, MN). The level of GAPDH gene expression served as an internal control.

Antibodies

Monoclonal antibody against β-actin (Sigma) was used to standardize cytosolic protein loading on the SDS-PAGE. Anti-cytochrome *c* oxidase subunit IV (COX4) antibody (Molecular Probes, Eugene, OR) was used to standardize the mitochondrial protein levels. COX4 is a membrane protein in the inner mitochondrial membrane and it remains in the mitochondria regardless of activation of apoptosis. Antibodies against α-spectrin (Affiniti, Exeter, UK) and phospho-p38 MAPK (Promega, Madison, WI) were also used. Antibodies against MT1 and MT2 were purchased from Santa Cruz Biotech (Santa Cruz, CA). All other primary antibodies were purchased from Santa Cruz Biotech or Calbiochem (Gibbstown, NG). Secondary antibodies were horseradish peroxidase-conjugated goat anti-mouse IgG (ICN Biomedicals, Aurora, OH) and horseradish peroxidase-conjugated goat anti-rabbit IgG (ICN Biomedicals, Solon, OH).

Western blotting

The isolation of cytosolic, mitochondrial, and nuclear fractions were performed by standard procedures [34–36]. Western blotting was performed as described previously [34–36] and was used to analyze cytochrome *c* in the supernatants and pellets and CAD in nuclear fractions. The films were scanned using Photoshop software (Adobe Systems, Seattle, WA) and optical density (OD) of each band was determined using Quantity One software (Bio-Rad, Hercules, CA).

Detection of reactive oxygen species and mitochondrial membrane potential

The fluorescent probe 2′,7′-dichlorofluorescin diacetate (DCF-DA) was used for the assessment of intracellular reactive oxgen species (ROS) production in VSC4.1 cells in different treatment conditions, as described previously [36]. Briefly, cells were seeded (2×10^5 cells/well) in 6-well culture plates. On the second day afterseeding, cells were treated with different concentrations of H_2O_2, LGA, and TNF-α and with melatonin or melatonin + luzindole. Cells were then incubated at 37°C for 30 to 1440 min. After each time point (30 – 1440 min), plates were washed twice with Hank's balanced salt solution (GIBCO-BRL, Grand Island, NY) and loaded with 1000 μl DMEM/F12 containing 5 μM of DCF-DA. The fluorescence intensity was measured at 530 nm after excitation at 480 nm in Spectramax Gemini XPS (Molecular Devices, Sunnyvale, CA) and the increase in fluorescence intensity was used to assess the generation of net intracellular ROS.

Mitochondrial potential loss was measured by using fluorescent probe JC-1. Control and treated cells were incubated in DMEM/F12 medium containing 5 μg/ml JC-1 during treatment from 1 h to 24 h (60 min to 1440 min). After staining, the cultures were washed twice with PBS (pH 7.4). When excited at 488 nm, the fluorescence emission of JC-1 was measured at wavelengths corresponding to its monomer (530 ± 15 nm) and *J* aggregate (>590 nm) forms. Fluorescencewas measured in a fluorescent plate reader (Molecular Devices, Sunnyvale, CA)

Colorimetric assays for the measurement of caspase-8, caspase-9, and caspase-3 activities

Caspase activities in cells were measured with commercially available caspase-8 (Abcam, Cambridge, MA), caspase-9 (Abcam), and caspase-3 assay kits (Sigma). The colorimetric assays were based on the hydrolysis of the Ac-IETD-*p*NA by caspase-8, Ac-LEHD-*p*NA by caspase-9, and Ac-DEVD-*p*NA by caspase-3, resulting in the release of the *p*-nitroaniline (*p*NA). Proteolytic reactions were carried out in extraction buffer containing 200 μg of cytosolic protein extract and 40 μM Ac-IETD-*p*NA, 40 μM Ac-LEHD-*p*NA, or 40 μM Ac-DEVD-*p*NA. The reaction mixtures were incubated at room temperature for 2 h and the formation of *p*NA was measured at 405 nm in a colorimeter. The concentration of the *p*NA released from the substrate was calculated from the absorbance values. Experiments were performed in triplicate.

Statistical analysis

Results obtained from different treatments were analyzed using StatView software (Abacus Concepts). Data are expressed as mean ± standard error of mean (SEM) of separate experiments (n>3) and compared by one-way analysis of variance (ANOVA) followed by Fisher's post-hoc test. Significant difference between control (CTL) and H_2O_2, LGA, TNF-α, or all luzindole treatments were indicated by * $P \leq 0.05$ or ** $P \leq 0.01$. Significant difference between H_2O_2, LGA, or TNF-α treatments and melatonin post-treatment (15 min) + H_2O_2, LGA, or TNF-α was indicated by $^{\#}P < 0.05$ or $^{\#\#}P < 0.01$. Significant difference between control (CTL) and melatonin treatments were indicated by • $P \leq 0.05$ or •• $P \leq 0.01$.

Results

The viability of VSC4.1 motoneurons was evaluated under a light microscope using trypan blue dye exclusion test (Fig. 1A). Melatonin at 15 min post-treatment of cells in the presence of H_2O_2, or LGA, or TNF-α maintained cell viability (Fig. 1A). In order to determine functional neuroprotection, whole-cell membrane potentials were recorded by patch-clamp technique in VSC4.1 cells following all treatments (Fig. 1B). Cells treated with melatonin and luzindole alone caused no significant difference in the membrane potentials compared with control. A majority of H_2O_2, LGA, TNF-α, or melatonin + luzindole-treated cells underwent cell death, and thus, membrane potentials could not be recorded. There was no significant difference in membrane potentials between control cells and cells exposed to H_2O_2, LGA, or TNF-α and then treated with melatonin ($P = 0.768$), indicating similar electrophysiological function of these cells and efficacy of melatonin in preserving neuronal functionality.

Morphological features of apoptosis were detected following Wright staining (Fig. 2A). Apoptotic death was confirmed based on the characteristic morphological features such as condensation of the nucleus and cytoplasm, cytoplasmic blebbing, and the formation of apoptotic bodies. Results obtained from Wright staining were further supported by the ApopTag assay (Fig. 2B). Both control and melatonin-treated cells showed little or no brown color, confirming almost absence of ApopTag-positive cells or apoptosis. All treatment groups were examined under the light microscopy and cells were counted to determine the percentage of apoptotic cells (Fig. 2). Compared with control cells, cells treated with 50 μM H_2O_2, 25 μM LGA, 50 ng/ml TNF-α, or (H_2O_2 or LGA, or TNF-α) + melatonin + luzindole (a melatonin receptor antagonist) showed an increase ($P < 0.05$) in (more than 50%) apoptotic cells (Fig. 2C). At 15 min post-treatment of cells with 150 nM melatonin, there was a decrease in 50 μM H_2O_2, 25 μM LGA, and 50 ng/ml TNF-α-induced apoptosis by 3 to 4-fold, compared with treatment of cells with 50 μM H_2O_2, 25 μM LGA,

and 50 ng/ml TNF-α only. Therefore, melatonin receptor antagonist luzindole prevented melatonin-mediated protection of cells.

To ascertain whether the VSC4.1 motoneurons used in these experiments expressed melatonin receptors (MT1 and MT2) at the mRNA and protein levels, we performed RT-PCR using rat specific primers (Table 1) and Western blotting using specific antibodies. We examined mRNA expression of specific genes (Fig. 3A). When the RNA samples from cells treated with 100 nM melatonin was processed without reverse transcription, no amplified products were detected indicating RT-PCR specificity and the absence of DNA contamination. The level of GAPDH gene expression served as an internal control. While our results indicated the presence of MT1 and MT2 in VSC4.1 motoneurons, the mRNA expression level of MT1 was greater in melatonin-treated cells (Fig. 3A, B). The level of expression of MT2 was less than level of expression of MT1. We also detected higher expression of MT1 at the mRNA level in melatonin only treated cells than post-treatment of cells with melatonin (Fig. 3A, B). Cells treated with H_2O_2, LGA, or TNF-α alone and with each in presence of melatonin + luzindole showed significantly reduced levels of MT1 (2-fold at both mRNA and protein levels) and MT2 (1.5-fold at mRNA levels), compared with untreated cells. Post-treatment with melatonin restored melatonin receptor MT1 expression at protein level in cells exposed to H_2O_2, LGA, or TNF-α (Fig. 3C, D), while the expression was decreased in the presence of melatonin receptor antagonist. No significant changes were seen in MT2 expression at the protein levels in the presence or absence of melatonin or its receptor antagonist.

To examine the possibility of ROS inhibition by melatonin, we measured fluorescence intensity (as a measure of ROS production) resulting from the oxidation of dichlorofluorescin (DCF) in VSC4.1 cells in a time-dependent manner. All cytotoxic agents promoted the oxidation of DCF in VSC4.1 cells and melatonin completely blocked increases in ROS production (Fig. 4A). The results demonstrated that melatonin acts as a potent antioxidant by inhibiting ROS production. Since ROS could act as important signaling molecules for activation of mitogen-activated protein kinases (MAPKs), we determined the expression levels of 38 kD p-p38 MAPK and 46 kD p-JNK1 kinases. Our results showed significant increases in p38 MAPK and JNK1 phosphorylation in VSC4.1 cells after treatments with H_2O_2, LGA, or TNF-α (Fig. 4B, C). Melatonin completely blocked the increases in phosphorylation of p38 MAPK (Fig. 4C) and JNK1, indicating the involvement of ROS in triggering the generation of phosphorylated p38 MAPK and JNK1. There was no change in p38 MAPK under above conditions. Also, treatment with luzindole significantly decreased the ability of melatonin effect by increasing ROS production and activation of p38 MAPK and JNK1 kinases.

In order to investigate the effect of melatonin on extrinsic pathways of apoptosis, caspase-8 activation was examined in VSC4.1 cells. Our results showed significant increase in 18 kD caspase-8 active bands in VSC4.1 cells treated with H_2O_2 ($P = 0.023$), LGA ($P = 0.013$), or TNF-α ($P = 0.001$) (Fig. 5A). β-Actin expression was monitored to ensure that equal amounts of protein were loaded in each lane. Caspase-8 activation induced the proteolytic cleavage of Bid to tBid, which could translocate from cytosol to mitochondrial membrane to stimulate more efficient oligomerization of Bax and thereby activation of the intrinsic apoptotic pathway. The levels of tBid were determined in mitochondrial fraction by Western blotting and were significantly increased in cells treated with cytotoxic agents. COX4 was used as a mitochondrial internal control. We found melatonin completely blocked caspase-8 activation and proteolytic cleavage of Bid to tBid significantly in VSC4.1 cells treated with H_2O_2, LGA, or TNF-α (Fig. 5A, B) and post-treatment with luzindole significantly decreased the melatonin action. Caspase-8 activation was significantly increased in these

cells following treatment with cytotoxic agents. Melatonin attenuated increase in caspase-8 activity and melatonin receptor antagonist reversed the melatonin effect (Fig. 5C).

Melatonin's interference with the intrinsic pathway of apoptosis at the mitochondrial level was examined. Treatment of cells with H_2O_2, LGA, or TNF-α increased Bax but decreased Bcl-2 expression at mRNA and protein levels (Fig. 6A, B). The Bax:Bcl-2 ratio, as determined by Western blotting, was significantly increased following treatments (Fig. 6C). Cells treated with H_2O_2, LGA, or TNF-α showed a significant ($P = 0.004$) 3-fold increase in the Bax:Bcl-2 ratio, compared with control cells (Fig. 6C). Examination of mRNA expression by RT-PCR showed that treatment with H_2O_2, LGA, or TNF-α increased bax levels and decreased bcl-2 levels while GAPDH levels remained uniform in all treatments (Fig. 6A). We used a monoclonal antibody that recognized 21 kD Baxα and 24 kD Baxβ isoforms and another antibody that detected 26 kD Bcl-2 on the Western blots. Treatment of VSC4.1 motoneurons with H_2O_2, LGA, or TNF-α increased total Bax expression (Fig. 6B), resulting an increase in Bax:Bcl-2 ratio (Fig. 6C) to promote mitochondrial release of pro-apoptotic factors. Melatonin treatment significantly ($P = 0.013$) attenuated increase in Bax:Bcl-2 ratio, compared with cells treated with cytotoxic agents. Also, there was no significant difference between control cells and cells exposed to H_2O_2, LGA, or TNF-α and then post-treated with melatonin ($P = 0.411$). Melatonin treatment alone did not significantly alter the Bax:Bcl-2 ratio ($P = 0.545$).

Mitochondrial swelling is often associated with the loss of mitochondrial membrane potential ($\Delta\psi m$), a phenomenon readily measured after staining with the mitochondrial dye JC-1. As expected, control cells showed a high JC-1 ratio (590 nm/530 nm) after staining of VSC 4.1 cells with JC-1. After H_2O_2, LGA, or TNF-α treatment, the mean red and green fluorescence ratios of the mitochondria dropped slowly in a biphasic way, indicating that the $\Delta\psi m$ had collapsed during apoptosis (Fig. 6D). This loss of membrane potential was associated with the disappearance of 15 kD cytochrome *c* from the mitochondrial fraction and its subsequent appearance in the cytosolic fraction (Fig. 6E). The expression of COX4 as an internal control was monitored in mitochondrial fraction. The mitochondrial release of cytochrome *c* into the cytosol could cause activation of caspase-9 (Fig. 6E, F). We detected an increase in active 37 kD caspase-9 fragment in VSC4.1 cells following treatment with H_2O_2, LGA, or TNF-α. The cytosolic fraction was used to examine β-actin expression to ensure that equal amount of protein was loaded in each lane. Further, colorimetric assay using a chromogenic synthetic substrate showed significant increase in caspase-9 activity in VSC4.1 cells after treatment with H_2O_2, LGA, or TNF-α (Fig. 6G). Post-treatment of melatonin significantly blocked mitochondrial potential by preventing mitochondrial release of cytochrome *c* and subsequent inhibition of caspase-9 activation. Further, treatment with luzindole significantly decreased the ability of melatonin action.

Intracellular free [Ca^{2+}] was determined in all treatment groups using fura-2 assay (Fig. 7A). Cells treated for 24 h with H_2O_2, LGA, or TNF-α demonstrated a significant increase, more than 2–2.5 fold ($P = 0.008$), in intracellular [Ca^{2+}] level when compared with control cells. This increase was attenuated by 70% ($P = 0.009$) due to post-treatment with melatonin. Furthermore, there was no significant difference ($P = 0.387$) between intracellular [Ca^{2+}] concentrations in control cells and cells treated with H_2O_2, LGA, or TNF-α plus melatonin (Fig. 7). No significant difference ($P = 0.611$) was seen between control cells and cells treated with melatonin alone. The increase in Ca^{2+} concentration suggests the possibility of activation of the Ca^{2+}-dependent protease calpain in course of cell death. Thus, the levels of calpain (Fig. 7B, C) caspse-3 (Fig. 7B, C, D) expression and activation and also their roles in apoptosis of VSC4.1 cells were determined. Calpain and caspase-3 were overexpressed in cells treated with cytoxic agents (Fig. 7B, C). Degradation of 270 kD α-spectrin to 145 kD spectrin breakdown product (SBDP) and 120 kD SBDP was taken as a measure of

proteolytic activity of calpain and caspase-3, respectively. Cells treated with H_2O_2, LGA, or TNF-α produced greater amount of 145 kD SBDP and 120 kD SBDP (Fig. 7B, C), indicating increased activities of calpain and caspase-3, respectively. A colorimetric assay showed very significant increases in total caspase-3 activity in VSC4.1 cells after exposure to H_2O_2, LGA, or TNF-α (Fig. 7D). This cytoxic agent-mediated increases in both calpain and capase-3 activity were significantly ($P \leq 0.001$) attenuated by post-treatment with melatonin. The melatonin-mediated effects on proteolytic activities were reversed by luzindole (Fig. 7B, C, D). Increased activity of caspase-3 also cleaved the inhibitor of caspase-activated DNase (ICAD), causing release and translocation of caspase-activated DNase (CAD) to the nucleus (Fig. 7E, F) to cause degradation of nuclear DNA. Post-treatment of melatonin significantly blocked the ICAD degradation and subsequent translocation of CAD to the nucleus. Further, treatment of luzindole significantly decreased the ability of melatonin action. Uniform expression of β-actin served as a loading control for cytosolic proteins. We stained one set of gel with Coomassie Blue to ensure loading of equal amounts of nuclear proteins in all lanes (Fig. 7E).

Discussion

Melatonin is a powerful antioxidant, which scavenges the highly toxic hydroxyl radicals as well as other species that initiate lipid peroxidation, DNA damage, and protein oxidation via receptor-and non-receptor-mediated pathways. However, the results obtained from this study suggest that melatonin-mediated cytoprotection via a receptor-mediated pathway is due to inhibition of calpain and caspases-mediated proteolytic pathways involved in cell death (Fig. 1). The present results support a direct relationship between cytoprotection and inhibition of kinases (p-p38 MAPK and p-JNK1) and protease activities (calpain and caspase-3). Melatonin prevents ROS production, Ca^{2+} influx, and cell death induced by oxidative stress, glutamate excitotoxcity, and TNF-α toxicity in VSC4.1 motoneurons, strongly indicating involvement of multiple mechanisms. Post-treatment with luzindole significantly decreased the ability of melatonin to protect cells, indicating the involvement of melatonin receptor in providing melatonin-mediated neuroprotection. Thus, these results showed that melatonin worked via its receptors to prevent apoptosis in VSC4.1 motoneurons.

Recent findings indicate that the G protein-coupled melatonin receptors termed MT1 and MT2 (also known as Mel1a and Mel1b, respectively) are expressed in neurons of the brain in mammals including humans [37–42], and that these receptors mediate the physiological actions of melatonin [43–44]. Hence, the contribution of various melatonin receptors to the neuroprotection mechanism was analyzed. The current investigations indicate that both melatonin receptors (MT1 and MT2) are expressed in VSC4.1 motoneurons, but MT2 expression is negligible (at protein level). The increase in expression of MT1 and MT2 at mRNA levels in melatonin-treated cells was substantial (Fig. 3). Our studies showed that pharmacological concentrations of melatonin are needed to protect VSC4.1 motoneurons from H_2O_2, LGA, or TNF-α-induced cell death indicating that protection rendered by melatonin might be via its receptor-mediated pathway. The neuroprotective effect of melatonin and their receptors was further confirmed by determining the recovery of membrane potential of these cells suggesting that melatonin restored neuronal function. This contention is supported by the fact that luzindole, a melatonin receptor antagonist, abrogated the neuroprotection and functionality of cells provided by melatonin.

On the basis of the present results and the previously published data, melatonin receptors have been shown to inhibit several signal transduction cascades, including formation of cAMP, mobilization of Ca^{2+}, release of arachidonic acid, and synthesis of diacylglycerol [45]. Thus, the effects of melatonin are clearly not limited to its hypothetical direct free radical-scavenging ability and suggest that melatonin may signal through a variety of

regulated pathways. Our observation showed that post-treatment of melatonin decreased ROS production (Fig. 4A), which may suggest an antioxidant effect of this substance with a possible underlying role in mitochondrial protection and anti-apoptotic signaling. Normally, cells respond to oxidative stress injury by activation of several pathways including the activation of stress-activated MAP kinases (SAPKs). A large number of studies [46] and our present results demonstrate that cell injury is associated with phosphorylation of p38 MAPK and c-Jun N-terminal kinase (JNK) (Fig. 4B, C). Post-treatment with melatonin blocks this effect. These results suggest that melatonin protect against H_2O_2, LGA, or TNF-α-induced cell death by suppressing ROS-mediated p38 MAPK and JNK-1 pathways.

In the extrinsic pathways of cell death mechanism, caspase-8 is required before mitochondrial permeabilization and release of cytochrome *c* [47]. To investigate the mechanisms involved in cell protection by melatonin that regulates initial caspase-8 activation and Bid cleavage and translocation to mitochondria during apoptosis, we first detected the inhibition of caspase-8 and Bid cleavage in melatonin-treated cells. The activation of caspase-8 was found to be more than 3-fold in the TNF-α-treated cells when compared with cells exposed H_2O_2 or LGA (Fig. 5). These results suggested that TNF-α processing of caspase-8 (degradation of procaspase-8 and appearance of active caspase-8) was greater in VSC4.1 motoneurons, compared with H_2O_2 or LGA processing. Since mitochondria playa key role both in maintaining cellular homeostasis and in triggering the activation of cell death pathways, we evaluated the effect of melatonin on expression of pro-apoptotic Bax and anti-apoptotic Bcl-2 and alterations of mitochondrial transmembrane potential ($\Delta\psi_m$) as well as release of cytochrome *c* in H_2O_2, LGA, or TNF-α-treated cells [29]. Our results show that melatonin can protect apoptotic cells by inhibiting the alteration of bax or bcl-2 at mRNA and protein levels of Bax and Bcl-2, which also indicates a decrease in the Bax:Bcl-2 ratio (Fig. 6A, B, C). The present study also demonstrated that melatonin prevented loss of mitochondrial membrane potential, release of mitochondrial factors, and activation of caspase-9 (Fig. 6D, E, F), leading to the protection of cells from damage and restored cell function. Apart from protecting cells from ROS-dependent events, melatonin showed a variety of beneficial actions at the mitochondria level.

Abnormal Ca^{2+} influx in cellular compartments [34,42] causes activation of a number of Ca^{2+}-dependent degradative processes, which are detrimental to cell survival. Our data suggest that melatonin suppresses the Ca^{2+} influx in VSC4.1 motoneurons following H_2O_2, LGA, or TNF-α exposure, which consequently may prevent the activation of Ca^{2+} -dependent events that are known to cause cell death. While the exact mechanism of action for melatonin in attenuating Ca2+ influx in VSC4.1 motoneurons exposed to H_2O_2, LGA, or TNF-α is not known, there are several examples in other cell types where melatonin-mediated influence on intracellular free [Ca^{2+}] and neuroprotection rendered by inhibition of both mitochondrial and ER [endoplasmic reticulum] pathways [48] or direct binding to calreticulin also has been suggested [49]. The observation that treatment with H_2O_2, LGA, or TNF-α alone leads to an increase in calpain and caspase-3 activity is in agreement with the results of previous studies [42]. We found that H_2O_2, LGA, or TNF-α increased the activation of caspase-3 activity and the levels of cleavage of ICAD (DFF45) in VSC4.1 cells. ICAD is a caspase-3 substrate that has to be cleaved before apoptotic internucleosomal DNA fragmentation can proceed. CAD (DFF40) remains inactive while bound to ICAD; however, caspase-3 cleaves ICAD at two sites, thereby releasing this endonuclease, which is then thanslocated to nucleus to cleave DNA [36]. From our own observations, decreases in calpain and caspase-3 activititis correlate well with reduction in the Bax:Bcl-2 ratio. Pro-apoptotic Bax is upstream of the caspases in the mitochondria-mediated apoptotic death pathway. These findings, taken together, support that melatonin-mediated cytoprotection is due, in part, to inhibition of the mitochondrial apoptotic pathway as reported earlier [42].

Our results indicate that melatonin post-treatment inhibits oxidative damage, glutamate excitotoxicity, and TNF-α mediated VSC4.1 cell death. Further, melatonin post-treatment can be associated with an increase in MT1 and MT2 expression. The results reported here also showed that the inhibitory effects of melatonin on VSC4.1 cells were prevented by luzindole, suggesting the neuroprotective effect was produced by activation of MT1 and MT2 receptors. This seems to argue in favor of a receptor-mediated effect of melatonin for rendering neuroprotection. Our results indicate that the cytoprotective effects of melatonin may be in part due to reduction of Ca^{2+} influx and activation of calpain and caspase-3 following oxidative stress and glutamate exitotoxicity and. Thus, our data suggest that the multi-active agent melatonin may have a significant role in neuroprotection in mutifactorial CNS injuries and diseases. In conclusion, we present substantial evidence that antioxidant properties of melatonin are involved in its neuroprotective effect against oxidative damage, glutamate excitotoxicity and TNF-α toxicity in VSC 4.1 cells and thus melatonin can be used as a potential therapeutic agent for the treatment of CNS injuries and various neurodegenerative diseases.

Acknowledgments

This investigation was supported in part by the R01 grants from the NINDS (NS-31622, NS-41088, NS-45967, and NS-57811), NCI (CA-91460), and NIH (C06 RRO15455).

References

1. HARDELAND R. Melatonin: signaling mechanisms of a pleiotropic agent. Biofactors. 2009; 35:183–192. [PubMed: 19449447]
2. REITER RJ, TAN DX, MANCHESTER LC, et al. Medical implications of melatonin: receptor-mediated and receptor-independent actions. Adv Med Sci. 2007; 52:11–28. [PubMed: 18217386]
3. MARTIN M, MACIAS M, ESCAMES G, et al. Melatonin but not vitamins C and E maintains glutathione homeostasis in t-butyl hydroperoxide-induced mitochondrial oxidative stress. FASEB J. 2000; 14:1677–1679. [PubMed: 10973915]
4. JOU MJ, Peng TI, Yu PZ, et al. Melatonin protects against common deletion of mitochondrial DNA-augmented mitochondrial oxidative stress and apoptosis. J Pineal Res. 2007; 43:389–403. [PubMed: 17910608]
5. REITER RJ, PAREDES SD, KORKMAZ A, et al. Melatonin combats molecular terrorism at the mitochondrial level. Interdisc Toxicol. 2008; 1:137–149.
6. TAN DX, CHEN LD, POEGGELER B, et al. Melatonin: A potent, endogenous hydroxyl radical scavenger. Endocr J. 1993; 1:57–60.
7. CARRILLO-VICO A, GARCIA-MAURINO S, CALVO JR, et al. Melatonin counteracts the inhibitory effect of PGE2 on IL-2 production in human lymphocytes via its mt1 membrane receptor. FASEB J. 2003; 17:755–757. [PubMed: 12594180]
8. TAMURA EK, CECON E, MONTEIRO AW, et al. Melatonin inhibits LPS-induced NO production in rat endothelial cells. J Pineal Res. 2009; 46:268–274. [PubMed: 19215575]
9. HILL SM, BLASK DE. Effects of the pineal hormone melatonin on the proliferation and morphological characteristics of human breast cancer cells (MCF-7) in culture. Cancer Res. 1988; 48:6121–6126. [PubMed: 3167858]
10. JOO SS, YOO YM. Melatonin induces apoptotic death in LNCaP cells via p38 and JNK pathways: therapeutic implications for prostate cancer. J Pineal Res. 2009; 47:8–14. [PubMed: 19522739]
11. SAINZ RM, MAYO JC, URIA H, et al. The pineal neurohormone melatonin prevents in vivo and in vitro apoptosis in thymocytes. J Pineal Res. 1995; 19:178–188. [PubMed: 8789249]
12. MARTIN V, SAINZ RM, ANTOLIN I, et al. Several antioxidant pathways are involved in astrocyte protection by melatonin. J Pineal Res. 2002; 33:204–212. [PubMed: 12390502]
13. MANDA K, UENO M, ANZAI K. Cranial irradiation-induced inhibition of neurogenesis in hippocampal dentate gyrus of adult mice: attenuation by melatonin pretreatment. J Pineal Res. 2009; 46:71–78. [PubMed: 18798786]

14. MAYO JC, SAINZ RM, URIA H, et al. Inhibition of cell proliferation: a mechanism likely to mediate the prevention of neuronal cell death by melatonin. J Pineal Res. 1998; 25:12–18. [PubMed: 9694399]
15. HERRERA F, SAINZ RM, MAYO JC, et al. Glutamate induces oxidative stress not mediated by glutamate receptors or cystine transporters: protective effect of melatonin and other antioxidants. J Pineal Res. 2001; 31:356–362. [PubMed: 11703566]
16. BENI SM, KOHEN R, REITER RJ, et al. Melatonin-induced neuroprotection after closed head injury is associated with increased brain antioxidants and attenuated late-phase activation of NF-kappaB and AP-1. FASEB J. 2004; 18:149–151. [PubMed: 14597558]
17. JAHNKE G, MARR M, MYERS C, et al. Maternal and developmental toxicity evaluation of melatonin administered orally to pregnant Sprague-Dawley rats. Toxicol Sci. 1999; 50:271–279. [PubMed: 10478864]
18. COSTA EJ, LOPES RH, LAMY-FREUND MT, et al. Permeability of pure lipid bilayers to melatonin. J Pineal Res. 1995; 19:123–126. [PubMed: 8750345]
19. REITER RJ, TAN DX, PAPPOLLA MA. Melatonin relieves the neural oxidative burden that contributes to dementias. Ann N Y Acad Sci. 2004; 1035:179–196. [PubMed: 15681808]
20. LISSONI P, BUCOVEC R, BONFANTI A, et al. Thrombopoietic properties of 5-methoxytryptamine plus melatonin versus melatonin alone in the treatment of cancer-related thrombocytopenia. J Pineal Res. 2001; 30:123–126. [PubMed: 11270479]
21. LEÓN J, MACÍAS M, ESCAMES G, et al. Structure-related inhibition of calmodulin-dependent neuronal nitric-oxide synthase activity by melatonin and synthetic kynurenines. Mol Pharmacol. 2000; 58:967–975. [PubMed: 11040043]
22. PEYROT F, DUCROCQ C. Potential role of tryptophan derivatives in stress responses characterized by the generation of reactive oxygen and nitrogen species. J Pineal Res. 2008; 45:235–246. [PubMed: 18341517]
23. NATARAJASI M, SADEGHI K, REITER RJ, et al. The neurohormone melatonin inhibits cytokine, mitogen and ionizing radiation induced NF-κB. Biochem Mol Biol Int. 1995; 37:1063–1070. [PubMed: 8747536]
24. CHUANG JI, MOHAN N, MELTZ ML, et al. Effect of melatonin on NF-kappa-B DNA-binding activity in the rat spleen. Cell Biol Int. 1996; 20:687–692. [PubMed: 8969462]
25. BECKER-ANDRÉ M, WIESENBERG I, SCHAEREN-WIEMERS N, et al. Pineal gland hormone melatonin binds and activates an orphan of the nuclear receptor superfamily. J Biol Chem. 1994; 269:28531–28534. [PubMed: 7961794]
26. YUAN H, TANG F, PANG SF. Binding characteristics, regional distribution and diurnal variation of ^{125}I-iodomelatonin binding sites in the chicken brain. J Pineal Res. 1990; 9:179–191. [PubMed: 1964478]
27. POON AM, PANG SF. 2 ^{125}I-iodomelatonin binding sites in spleens of guinea pigs. Life Sci. 1992; 50:1719–1726. [PubMed: 1316983]
28. ANDRABI SA, SAYEED I, SIEMEN D, et al. Direct inhibition of the mitochondrial permeability transition pore: a possible mechanism responsible for anti-apoptotic effects of melatonin. FASEB J. 2004; 18:869–871. [PubMed: 15033929]
29. TAN DX, MANCHESTER LC, TERRON MP, et al. Melatonin as a naturally occurring co-substrate of quinone reductase-2, the putative MT3 melatonin membrane receptor: hypothesis and significance. J Pineal Res. 2007; 43:317–320. [PubMed: 17910598]
30. KILIC U, KILIC E, REITER RJ, et al. Signal transduction pathways involved in melatonin-induced neuroprotection after focal cerebral ischemia in mice. J Pineal Res. 2005; 38:67–71. [PubMed: 15617539]
31. KOH PO. Melatonin attenuates the focal cerebral ischemic injury by inhibiting the dissociation of pBad from 14-3-3. J Pineal Res. 2008; 44:101–106. [PubMed: 18078455]
32. KOH PO. Melatonin prevents the injury-induced decline of Akt/forkhead transcription factors phosphorylation. J Pineal Res. 2008; 45:199–203. [PubMed: 18312296]
33. COYLE JT, PUTTFARCKEN P. Oxidative stress, glutamate, and neurodegenerative disorders. Science. 1993; 262:689–695. [PubMed: 7901908]

34. DAS A, SRIBNICK EA, WINGRAVE JM, et al. Calpain activation in apoptosis of ventral spinal cord 4.1 (VSC4.1) motoneurons exposed to glutamate: calpain inhibition provides functional neuroprotection. J Neurosci Res. 2005; 81:551–562. [PubMed: 15968645]
35. DAS A, BANIK NL, RAY SK. Differentiation decreased telomerase activity in rat glioblastoma C6 cells and increased sensitivity to IFN-γ and taxol for apoptosis. Neurochem Res. 2007; 32:2167–2183. [PubMed: 17694433]
36. DAS A, BANIK NL, RAY SK. Garlic compounds generate reactive oxygen species leading to activation of stress kinases and cysteine proteases for apoptosis in human glioblastoma T98G and U87MG cells. Cancer. 2007; 110:1083–1095. [PubMed: 17647244]
37. BRUNNER P, SÖZER-TOPCULAR N, JOCKERS R, et al. Pineal and cortical melatonin receptors MT1 and MT2 are decreased in Alzheimer's disease. Eur J Histochem. 2006; 50:311–316. [PubMed: 17213040]
38. JIMENEZ-JORGE S, JIMENEZ-CALIANI AJ, GUERRERO JM, et al. Melatonin synthesis and melatonin-membrane receptor (MT1) expression during rat thymus development: role of the pineal gland. J Pineal Res. 2005; 391:77–83. [PubMed: 15978061]
39. SAVASKAN E, AYOUB MA, RAVID R, et al. Reduced hippocampal MT2 melatonin receptor expression in Alzheimer's disease. J Pineal Res. 2005; 38:10–16. [PubMed: 15617532]
40. THOMAS L, PURVIS CC, DREW JE, et al. Melatonin receptors in human fetal brain: 2-[^{125}I]iodomelatonin binding and MT1 gene expression. J Pineal Res. 2002; 33:218–224. [PubMed: 12390504]
41. SAMANTARAY S, DAS A, THAKORE NP, et al. Therapeutic potential of melatonin in traumatic central nervous system injury. J Pineal Res. 2009; 47:134–142. [PubMed: 19627458]
42. DAS A, BELAGODU A, REITER RJ, et al. Cytoprotective effects of melatonin on C6 astroglial cells exposed to glutamate excitotoxicity and oxidative stress. J Pineal Res. 2008; 45:117–124. [PubMed: 18373557]
43. DUBOCOVICH ML, RIVERA-BERMUDEZ MA, GERDIN MJ, et al. Molecular pharmacology, regulation and function of mammalian melatonin receptors. Front Biosci. 2003; 8:1093–1108.
44. WITT-ENDERBY PA, RADIO NM, DOCTOR JS, et al. Therapeutic treatments potentially mediated by melatonin receptors: potential clinical uses in the prevention of osteoporosis, cancer and as an adjuvant therapy. J Pineal Res. 2006; 41:297–305. [PubMed: 17014686]
45. CHAN AS, LAI FP, LORK, et al. Melatonin mt1 and MT2 receptors stimulate c-Jun N-terminal kinase via pertussis toxin-sensitive and -insensitive G proteins. Cell Signal. 2002; 14:249–257. [PubMed: 11812653]
46. PUIG B, GOMEZ-ISLA T, RIBE E, et al. Expression of stress-activated kinases c-Jun N-terminal kinase (SAPK/JNK-P) and p38 kinase (p38-P), and tau hyperphosphorylation in neurites surrounding Aβ plaques in APP Tg2576 mice. Neuropathol Appl Neurobiol. 2004; 30:491–502. [PubMed: 15488025]
47. LIN CF, Chen CL, Chang WT, et al. Sequential caspase-2 and caspase-8 activation upstream of mitochondria during ceramide and etoposide-induced apoptosis. J Biol Chem. 2004; 279:40755–40761. [PubMed: 15262979]
48. LIN AM, FANG SF, CHAO PL, et al. Melatonin attenuates arsenite-induced apoptosis in rat brain: involvement of mitochondrial and endoplasmic reticulum pathways and aggregation of alpha-synuclein. J Pineal Res. 2007; 43:163–171. [PubMed: 17645694]
49. MACÍAS M, ESCAMES G, LEON J, et al. Calreticulin-melatonin. An unexpected relationship. Eur J Biochem. 2003; 270:832–840. [PubMed: 12603316]

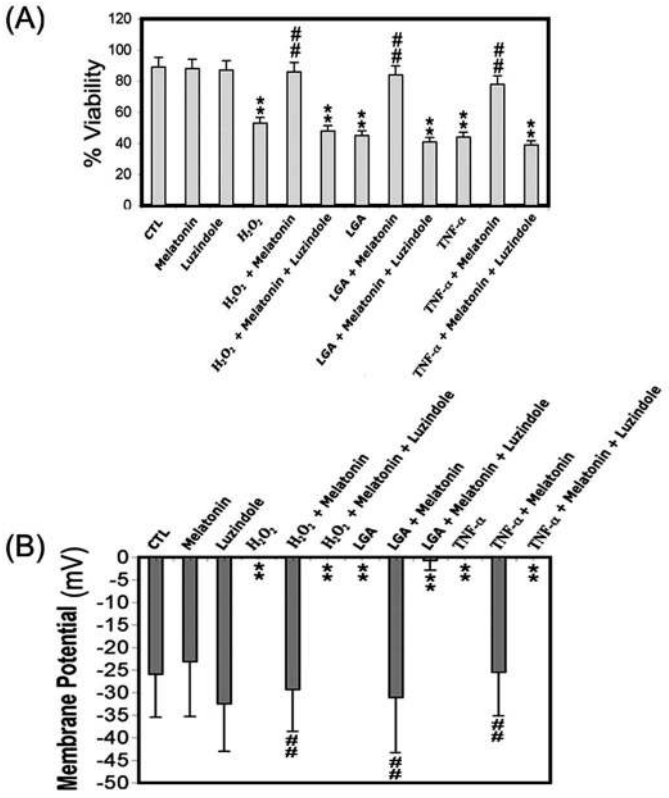

Fig. 1.

Post-treatment with melatonin prevented cell death and preserved functionality. (A) Post-treatment with melatonin prevented H_2O_2, LGA, or TNF-α mediated decrease in VSC4.1 cell viability. The trypan blue dye exclusion assay was used to assess cell viability in VSC4.1 cells. (B) Measurement of whole-cell membrane potential in VSC4.1 cells following treatments. Twelve treatment groups: control (CTL); 150 nM melatonin (24 h); 10 μM luzindole (24 h); 50 μM H_2O_2 (24 h); 50 μM H_2O_2 (24 h) + (15 min post-treat) melatonin; 50 μM H_2O_2 (24 h) + (15 min post-treat) melatonin + (20 min post-treat) luzindole; 25 μM LGA (24 h); 25 μM LGA (24 h) + post-treatment (15 min) of melatonin; 25 μM LGA (24 h) + (15 min post-treat) melatonin + (20 min post-treat) luzindole; 50 ng/ml TNF-α (24 h); 50 ng/ml TNF-α (24 h) + (15 min post-treat) melatonin; 50 ng/ml TNF-α (24 h) + (15 min post-treat) melatonin + (20 min post-treat) luzindole.

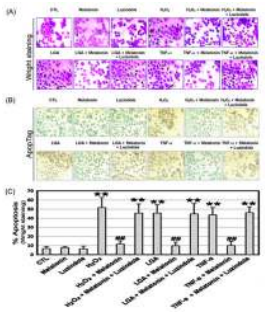

Fig. 2.

Post-treatment with melatonin prevented apoptotic death of VSC4.1 cells exposed to H_2O_2, LGA, or TNF-α. (A) Photomicrographs showing representative cells from each treatment group followingg Wright staining. The arrows indicate apoptotic cells. (B) Photomicrographs showing representative cells from each treatment group following ApopTag assay. (C) Bar graphs indicating the percentage of apoptotic cells in each group (based on Wright staining). Twelve treatment groups: control (CTL); 150 nM melatonin (24 h); 10 μM luzindole (24 h); 50 μM H_2O_2 (24 h); 50 μM H_2O_2 (24 h) + (15 min post-treat) melatonin; 50 μM H_2O_2 (24 h) + (15 min post-treat) melatonin + (20 min post-treat) luzindole; 25 μM LGA (24 h); 25 μM LGA (24 h) + post-treatment (15 min) of melatonin; 25 μM LGA (24 h) + (15 min post-treat) melatonin + (20 min post-treat) luzindole; 50 ng/ml TNF-α (24 h); 50 ng/ml TNF-α (24 h) + (15 min post-treat) melatonin; 50 ng/ml TNF-α (24 h) + (15 min post-treat) melatonin + (20 min post-treat) luzindole.

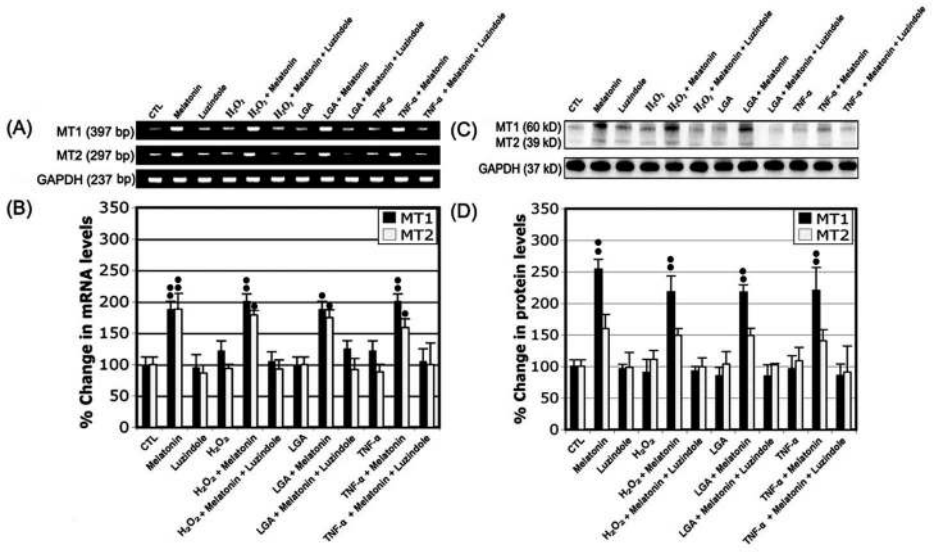

Fig. 3.

RT-PCR and Western blotting for determing expression of melatonin receptors in VSC4.1 cells. (A) Representative pictures to show levels of melatonin receptor 1 (MT1) and melatonin receptor 2 (MT2), and GAPDH at mRNA levels (RT-PCR). (B) Bar graphs to indicate the percentage of change in MT1 and MT2 expression relative to control (CTL) at mRNA level. (C) Representative pictures to show levels of MT1 and MT2, and β-Actin at protein levels (Western blotting). Twelve treatment groups: control (CTL); 150 nM melatonin (24 h); 10 μM luzindole (24 h); 50 μM H_2O_2 (24 h); 50 μM H_2O_2 (24 h) + (15 min post-treat) melatonin; 50 μM H_2O_2 (24 h) + (15 min post-treat) melatonin + (20 min post-treat) luzindole; 25 μM LGA (24 h); 25 μM LGA (24 h) + post-treatment (15 min) of melatonin; 25 μM LGA (24 h) + (15 min post-treat) melatonin + (20 min post-treat) luzindole; 50 ng/ml TNF-α (24 h); 50 ng/ml TNF-α (24 h) + (15 min post-treat) melatonin; 50 ng/ml TNF-α (24 h) + (15 min post-treat) melatonin + (20 min post-treat) luzindole.

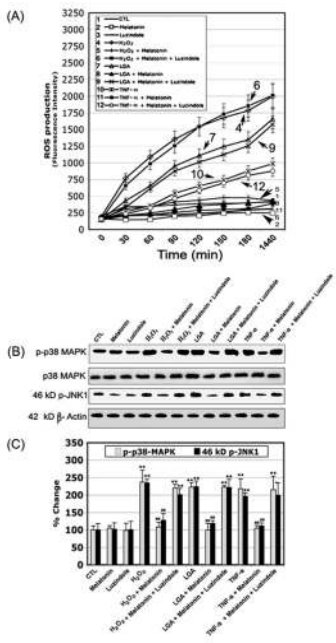

Fig. 4.

Determination of ROS production, p38 MAPK and JNK1 phosphorylation in VSC4.1 cells. (A) Inhibition of ROS production. Treatments (0, 30, 60, 90, 120, 150, 180, and 1440 min) in the presence of 5 μM 2,7-dichlorofluorescin diacetate (DCF-DA). (B) Western blotting to show levels of p-p38 MAPK, p38 MAPK, p-JNK-1 and β-actin. (C) Densitometric analysis showing percent change in optical density of the p-p38 MAPK and p-JNK-1 bands. Twelve treatment groups d: control (CTL); 150 nM melatonin (24 h); 10 μM luzindole (24 h); 50 μM H_2O_2 (24 h); 50 μM H_2O_2 (24 h) + (15 min post-treat) melatonin; 50 μM H_2O_2 (24 h) + (15 min post-treat) melatonin + (20 min post-treat) luzindole; 25 μM LGA (24 h); 25 μM LGA (24 h) + post-treatment (15 min) of melatonin; 25 μM LGA (24 h) + (15 min post-treat) melatonin + (20 min post-treat) luzindole; 50 ng/ml TNF-α (24 h); 50 ng/ml TNF-α (24 h) + (15 min post-treat) melatonin; 50 ng/ml TNF-α (24 h) + (15 min post-treat) melatonin + (20 min post-treat) luzindole.

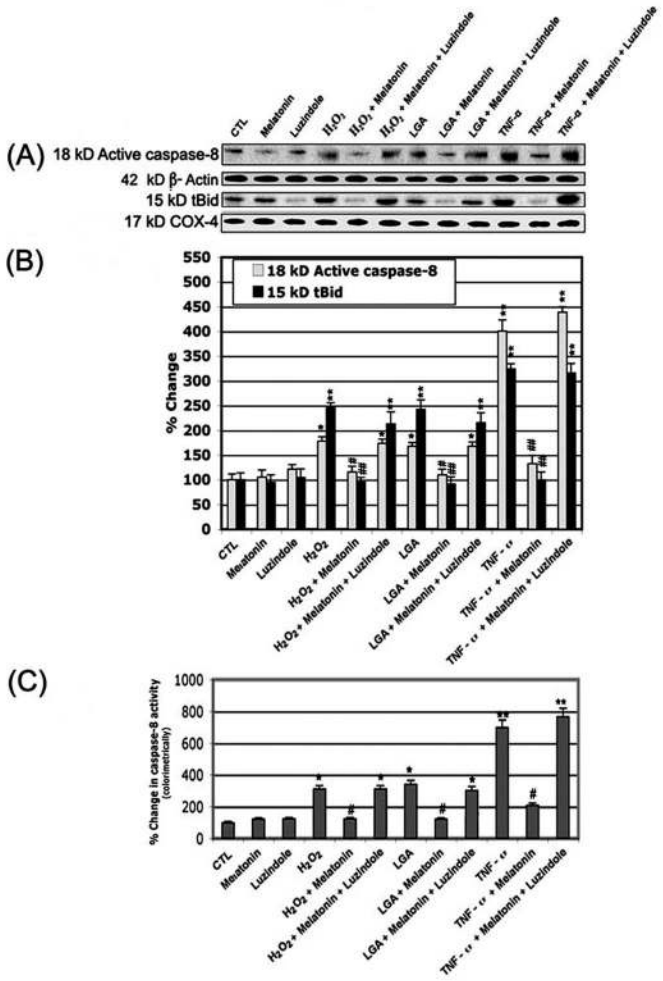

Fig. 5.

Determination of caspase-8 activation and Bid cleavage. (A) Western blotting to show levels of caspase-8, β-actin, tBid, and COX4. (B) Densitometric analysis to show percent change in optical density of the caspase-8 and tBid bands. (C) Colorimetric determination of caspase-8 activity. Twelve treatment groups: control (CTL); 150 nM melatonin (24 h); 10 μM luzindole (24 h); 50 μM H_2O_2 (24 h); 50 μM H_2O_2 (24 h) + (15 min post-treat) melatonin; 50 μM H_2O_2 (24 h) + (15 min post-treat) melatonin + (20 min post-treat) luzindole; 25 μM LGA (24 h); 25 μM LGA (24 h) + post-treatment (15 min) of melatonin; 25 μM LGA (24 h) + (15 min post-treat) melatonin + (20 min post-treat) luzindole; 50 ng/ml TNF-α (24 h); 50 ng/ml TNF-α (24 h) + (15 min post-treat) melatonin; 50 ng/ml TNF-α (24 h) + (15 min post-treat) melatonin + (20 min post-treat) luzindole.

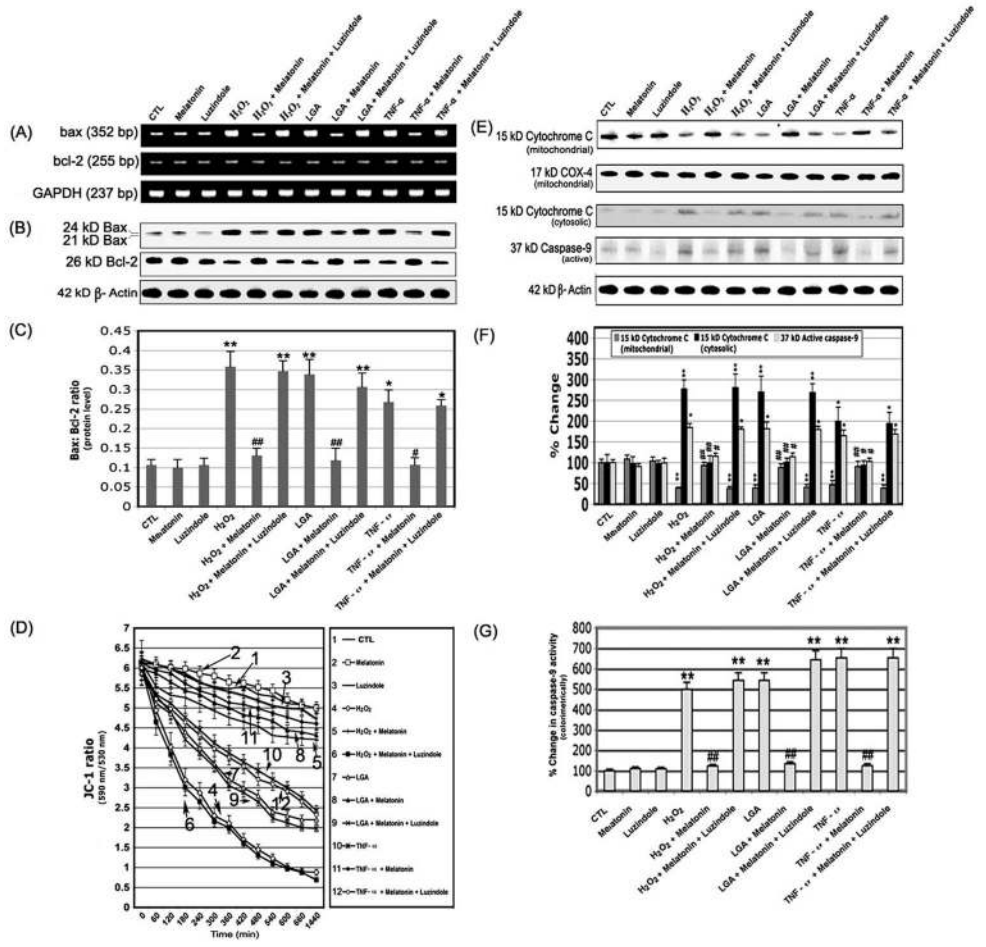

Fig. 6.

Examination of components involved in mitochondrial pathway of apoptosis in VSC4.1 cells. Alterations in Bax and Bcl-2 expression at mRNA and protein levels. Representative pictures to show Bax, Bcl-2, and GAPDH at (A) mRNA levels (RT-PCR) and (B) protein levels (Western blotting). (C) Densitometric analysis show the Bax:Bcl-2 ratio. (D) JC-1 ratio (590 nm/530 nm) in cells after the treatments for different times (30, 60, 120, 180, 240, 300, 360, 420, 480, 540, 600, 660, and 1440 min). (E) Western blotting for cytochrome *c*, COX4, caspase-9, and β-actin. (F) Densitometric analysis to show percent change in optical density of the mitochondrial and cytosolic 15 kD cytochrome *c* and 39 kD active caspase-9. (G) Determination of caspase-9 activity using a colorimetric assay. Twelve treatment groups: control (CTL); 150 nM melatonin (24 h); 10 μM luzindole (24 h); 50 μM H_2O_2 (24 h); 50 μM H_2O_2 (24 h) + (15 min post-treat) melatonin; 50 μM H_2O_2 (24 h) + (15 min post-treat) melatonin + (20 min post-treat) luzindole; 25 μM LGA (24 h); 25 μM LGA (24 h) + post-treatment (15 min) of melatonin; 25 μM LGA (24 h) + (15 min post-treat) melatonin + (20 min post-treat) luzindole; 50 ng/ml TNF-α (24 h); 50 ng/ml TNF-α (24 h) + (15 min post-treat) melatonin; 50 ng/ml TNF-α (24 h) + (15 min post-treat) melatonin + (20 min post-treat) luzindole.

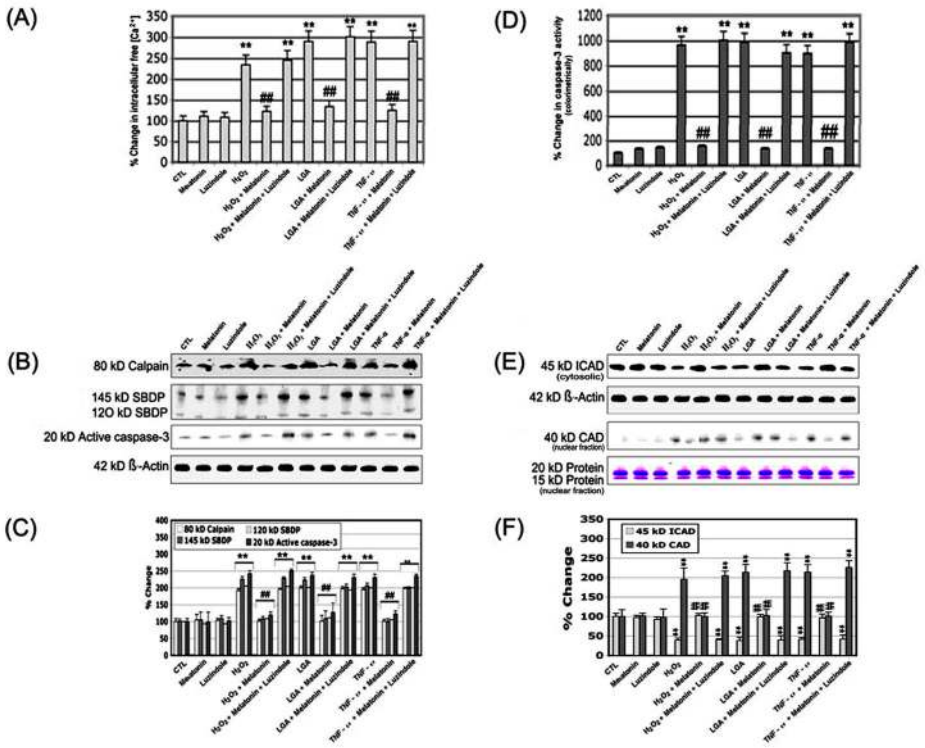

Fig. 7.

Examination of increase in intracellular free [Ca^{2+}], activation of calpain and caspase-3, and CAD. (A) Determination of intracellular free [Ca^{2+}]. (B) Western blotting to show levels of calpain, spectrin breakdown product (SBDP), and active caspase-3. (C) Densitometric analysis to document percent change in optical density of 80 kD calpain, 145 kD SBDP, 120 kD SBDP, and 20 kD caspase-3. (C) Determination of caspase-3 activity by a colorimetric assay. (E) Western blotting to show levels of ICAD, CAD, and β-actin. (F) Densitometric analysis to show percent change in optical density of the 45 kD ICAD, and 40 kD CAD. Twelve treatment groups:control (CTL); 150 nM melatonin (24 h); 10 μM luzindole (24 h); 50 μM H_2O_2 (24 h); 50 μM H_2O_2 (24 h) + (15 min post-treat) melatonin; 50 μM H_2O_2 (24 h) + (15 min post-treat) melatonin + (20 min post-treat) luzindole; 25 μM LGA (24 h); 25 μM LGA (24 h) + post-treatment (15 min) of melatonin; 25 μM LGA (24 h) + (15 min post-treat) melatonin + (20 min post-treat) luzindole; 50 ng/ml TNF-α (24 h); 50 ng/ml TNF-α (24 h) + (15 min post-treat) melatonin; 50 ng/ml TNF-α (24 h) + (15 min post-treat) melatonin + (20 min post-treat) luzindole. Das et al. (JPI-OM-10-09-0154)

Table 1

Primers used in RT-PCR for amplification of mRNA of specific genes

Gene	Primer sequences	Product size (bp)
GAPDH	Forward: 5′-TTC ACC ACC ATG GAG AAG GC-3′ Reverse: 5′-GGC ATG GAC TGT GGT CAT GA -3′	237
MT1	Forward: 5′-TGC TAC ATT TGC CAC AGT CTC-3′ Reverse: 5′-GAC CTA TGA AGT TGA GTG GGG-3′	397
MT2	Forward: 5′-TAC ATC AGC CTC ATC TGG CTT-3′ Reverse: 5′-CAC AAA CAC TGC GAA CAT GGT-3′	297
bax	Forward: 5′-GCA GAG AGG ATG GCT GGG GAG A-3′ Reverse: 5′-TCC AGA CAA GCA GCC GCT CAC G-3′	352
bcl-2	Forward: 5′-GGA TGA CTT CTC TCG TCG CTA C-3′ Reverse:5′-TGC AGA TGC CGG TTC AG-3′	255